

Wook Kang · Hee-Suk Jung

## Postbuckling of thin wood-based sandwich panels due to hygroexpansion under high humidity

Received: January 17, 2000 / Accepted: June 14, 2000

**Abstract** This study was carried out to investigate the postbuckling behavior of thin wood-based sandwich panels under high humidity. Using the Rayleigh–Ritz method based on the von Karman nonlinear theory for the panel, the solutions for both the approximate and the closed form for postbuckling of orthotropic panels were derived to evaluate the deflection for the boundary condition of all clamped edges. The results suggested that the edge movement be considered for evaluation of a critical moisture content and deflection of thin wood-based panels fixed on the core with an adhesive. The numerical solution obtained from the derived model showed some discrepancy with the experimental results. The predicted results overestimated the center deflection of the panels because creep and plastic deformation might be caused by considerable in-plane stress on panels.

**Key words** Postbuckling · Nonlinear theory · Orthotropic · Rayleigh-Ritz method · Plastic deformation

### Introduction

Most thin wood-based panels used for door skins, walls, and ceilings are attached to the core materials with nails or adhesives and are used for interior building applications and outdoor applications where the temperature and humidity fluctuate. The dimensional changes of these wood-based panels are likely due to moisture content (MC)

changes, which can go up a few percentage points within a day.<sup>1</sup> At a critical MC, the panel loses its dimensional stability, which leads to hygro buckling. The surface waviness of wood-based panels may be due to out-of-plane displacement after hygro buckling begins. This problem occurs often with the decorative panels coated with high glossy paint, which damages its decoration. Thus, it is necessary to understand this phenomenon on the basis of postbuckling theory.

Numerous studies on the buckling of laminated composite plates have been done, and Leissa<sup>2</sup> has provided an excellent review on the subject. For example, the postbuckling of anisotropic plates subjected to mechanical forces was studied by the Airy stress function and beam characteristic function in conjunction with both clamped and simply-supported boundary conditions.<sup>3</sup> A closed-form solution for simply-supported conditions and a finite element method for simply-supported and clamped conditions were reported for beam conditions.<sup>4</sup> Compared to those on mechanical forces, however, there are few studies on the thermal postbuckling behavior of laminated plates.<sup>5,6</sup> The closed-form approximate solution for orthotropic square plates with simply-supported edges were reported using the Rayleigh-Ritz method.<sup>7</sup> Studies on thermal postbuckling have made gradual progress in recent decades, but most of the studies focused on plates with simply-supported edges.<sup>8–12</sup>

From the literature review, the earlier studies on thermal postbuckling behavior could provide a tool for better understanding the postbuckling behavior of orthotropic plates. However, the earlier studies could not be used to predict postbuckling of orthotropic plates because the boundary conditions of wood-based sandwich panels are assumed to be clamped edges, and these panels also have movable edges owing to the expansion of facing panels.

To the authors' knowledge, the closed-form solution for orthotropic plates with clamped edges is not available. At the same time, few attempts have been made to find approximate solutions for columns. Moreover, some research has been done on the postbuckling of wood-based panels, such as that on strips.<sup>11</sup>

W. Kang (✉)

Institute of Forestry and Forest Products, College of Agriculture and Life Sciences, Seoul National University, 103 Seodun-Dong, Kwonsun-Gu, Suwon 441-744, Korea  
Tel. +82-331-290-2606; Fax +82-331-293-9376  
e-mail: kawook53@shinburo.com

H.-S. Jung

Department of Forest Products College of Agriculture and Life Sciences, Seoul National University, 103 Seodun-Dong, Kwonsun-Gu, Suwon 441-744, Korea

To optimize the structure of panel application, including the distance between the core material and surrounding conditions, this paper examined the hygropostbuckling behavior due to hygroexpansion of hollow-core wood-based sandwich panels composed of hardboards for the faces and laminated veneer lumber (LVL) for the core. The relation of hygroexpansion and stress in wood-based material is not elastic but is viscoelastic and mechanosorptive under moisture movement. This study was based on elastic behavior for the basic research.

For this purpose, both double sine series of the displacement function and the Rayleigh-Ritz method were employed to develop numerical models. The derived approximate solutions were compared to the experimental results of sandwich panels. The closed-form approximate solution for orthotropic panels was derived using only one term of a series for a reference.

## Theory

The total potential energy of an orthotropic panel<sup>13</sup> subjected to biaxial hygroexpansion forces is given as

$$\begin{aligned} \Pi = & \int_0^a \int_0^b \left[ \frac{1}{2} A_{11} \varepsilon_x^2 + A_{12} \varepsilon_x \varepsilon_y + \frac{1}{2} A_{22} \varepsilon_y^2 + \frac{1}{4} A_{66} \varepsilon_{xy}^2 \right. \\ & + \frac{1}{2} D_{11} \left( \frac{\partial^2 w}{\partial x^2} \right)^2 + D_{12} \frac{\partial^2 w}{\partial x^2} \frac{\partial^2 w}{\partial y^2} + \frac{1}{2} D_{22} \left( \frac{\partial^2 w}{\partial y^2} \right)^2 \\ & \left. + 2D_{66} \left( \frac{\partial^2 w}{\partial x \partial y} \right)^2 - N_x^M \varepsilon_x - N_y^M \varepsilon_y \right] dx dy \end{aligned} \quad (1)$$

where

$$\begin{aligned} N_x^M &= \Delta MC (\alpha_x A_{11} + \alpha_y A_{12}) \\ N_y^M &= \Delta MC (\alpha_x A_{21} + \alpha_y A_{22}) \end{aligned} \quad (2)$$

See Appendix for explanation of the abbreviations and symbols.

Nonlinear strains in midplane of panels defined by von Karman theory are given as

$$\begin{aligned} \varepsilon_x &= \frac{\partial u}{\partial x} + \frac{1}{2} \left( \frac{\partial w}{\partial x} \right)^2 \\ \varepsilon_y &= \frac{\partial v}{\partial y} + \frac{1}{2} \left( \frac{\partial w}{\partial y} \right)^2 \\ \gamma_{xy} &= \frac{1}{2} \varepsilon_{xy} = \frac{\partial v}{\partial x} + \frac{\partial u}{\partial y} + \frac{\partial w}{\partial x} \frac{\partial w}{\partial y} \end{aligned} \quad (3)$$

The stress-strain-moisture content relations for orthotropic panels is expressed as

$$\begin{bmatrix} \sigma_x \\ \sigma_y \end{bmatrix} = \begin{bmatrix} C_{11} & C_{12} \\ C_{21} & C_{22} \end{bmatrix} \begin{bmatrix} \varepsilon_x - \Delta MC \alpha_x \\ \varepsilon_y - \Delta MC \alpha_y \end{bmatrix} \quad (4)$$

There are four boundary conditions for all edges of the clamped panel,<sup>14</sup> but one was selected as shown as Eq. (5) for this work because it was consistent with immovable edges that were rigidly clamped to the panel.

$$\begin{aligned} w = 0, u = 0, v = 0, dw/dx = 0 \quad \text{for } x = 0, x = a \\ w = 0, u = 0, v = 0, dw/dy = 0 \quad \text{for } y = 0, y = a \end{aligned} \quad (5)$$

These assumed boundary conditions should be noted for comparison with other results. Deflection equations satisfying the above boundary condition in each direction are expressed as<sup>15</sup>

$$\begin{aligned} u &= \sum_{m=1}^{\infty} \sum_{n=1}^{\infty} A_{mn} \sin \frac{2m\pi x}{a} \sin \frac{(2n-1)\pi y}{b} (-1)^m (-1)^{n+1} \\ v &= \sum_{m=1}^{\infty} \sum_{n=1}^{\infty} B_{mn} \sin \frac{(2m-1)\pi x}{a} \sin \frac{2n\pi y}{b} (-1)^{m+1} (-1)^n \\ w &= \sum_{m=1}^{\infty} \sum_{n=1}^{\infty} C_{mn} \left( \cos \frac{2m\pi x}{a} - 1 \right) \left( \cos \frac{2n\pi y}{b} - 1 \right) (-1)^m (-1)^n \end{aligned} \quad (6)$$

The displacement functions can be obtained for an infinite strip,  $v = 0$ , by using Eq. (7) derived from Eq. (6)

$$\begin{aligned} u &= \sum_{m=1}^{\infty} A_m \sin \frac{2m\pi x}{a} (-1)^m \\ w &= \sum_{m=1}^{\infty} C_m \left( \cos \frac{2m\pi x}{a} - 1 \right) (-1)^m \end{aligned} \quad (7)$$

Substituting Eqs. (6) and (7) into Eq. (1), performing the integration, and minimizing the energy expression leads to Eq. (8).

$$\frac{\partial \Pi}{\partial A_{mn}} = 0, \quad \frac{\partial \Pi}{\partial B_{mn}} = 0, \quad \frac{\partial \Pi}{\partial C_{mn}} = 0 \quad (8)$$

Equation (8) gives simultaneous algebraic equations, which can be solved to obtain the Ritz coefficients,  $A_{mn}$ ,  $B_{mn}$ ,  $C_{mn}$ .

## Experiments

For construction of a test assembly, a hardboard panel with a density of 0.96 g/cm<sup>3</sup> was selected as facing material because it has been mainly used for door skins in industrial practice. The length/thickness ratios ( $alh$ ) were adjusted to 200:3, 300:3, and 400:3, respectively. The dimensions of the prepared panel ( $a \times b$ ) were 200 × 200 mm, 300 × 300 mm, and 400 × 400 mm with a constant thickness of about 3 mm. Specimens for determining the modulus of elasticity (MOE), dimensions, and moisture content (MC) changes were cut along the four edges of the buckling specimen. Linear expansion (LE), for which the span was 200 mm, was measured with digital Vernier calipers ( $\pm 0.01$  mm). The core material was laminated veneer lumber (LVL) made of radiata pine with a dimension of 26 × 30 mm (width × thickness). All the specimens cut from the

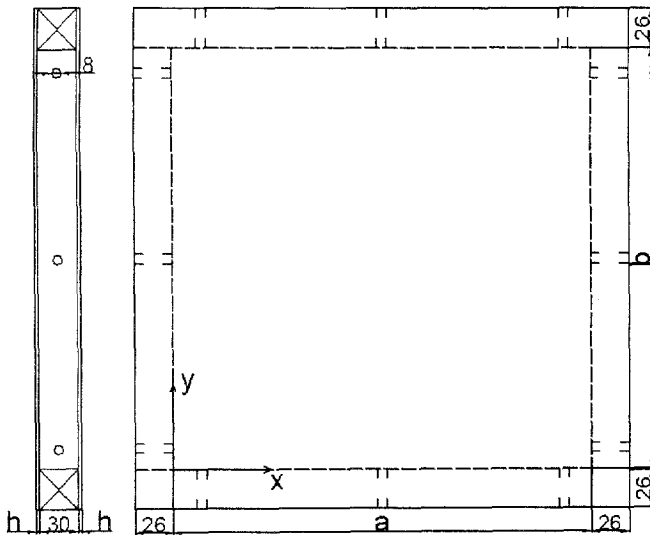


Fig. 1. Geometry of sandwich panel and assembly setup for test (units are millimeters)

panel were preconditioned at 25°C and 60% relative humidity (RH), which is below the indoor equilibrium moisture content (EMC). However, the core LVL was kept indoors and coated with oil-based paint to minimize the effect of the dimensional change on the test. As shown in Fig. 1, the square sandwich panels were symmetrically assembled with polyvinyl acetate (PVA) adhesive and were conditioned in a constant-humidity chamber of 25°C and 90% RH. Holes with an 8mm diameter was made at the middle of the core lumber to reduce the difference in the equilibrium rate between sample panels for buckling and dimensional change specimens. Strip specimens were fixed on the steel beam with a nut and bolt, which was enough to resist hygroexpansion forces. The center deflections of the sandwich panel and strip subjected to increasing relative humidity were measured at some intervals by a dial gauge (Fig. 1) and were compared with the numerical and analytical solutions derived. For the analysis, it was assumed that the MOE and the thickness change linearly with MC.

## Results and discussion

### Changes of MC and material properties

Figure 2 shows the changes of MC and LE as a function of time at 90% RH. It took about 130h for hardboard to reach an equilibrium state. Depending on the type of span used, the control specimens showed some variations in the changes of MC, thickness, linear expansion (LE), and MOE because they were cut from different panels (Table 1). The average changes of MC, thickness, and MOE were 4.6%, 4.3%, and 11.9%, respectively. The coefficients of LE for different span types ranged from  $0.397 \times 10^{-3}$  to  $0.461 \times 10^{-3}$  (average  $0.425 \times 10^{-3}$ ).

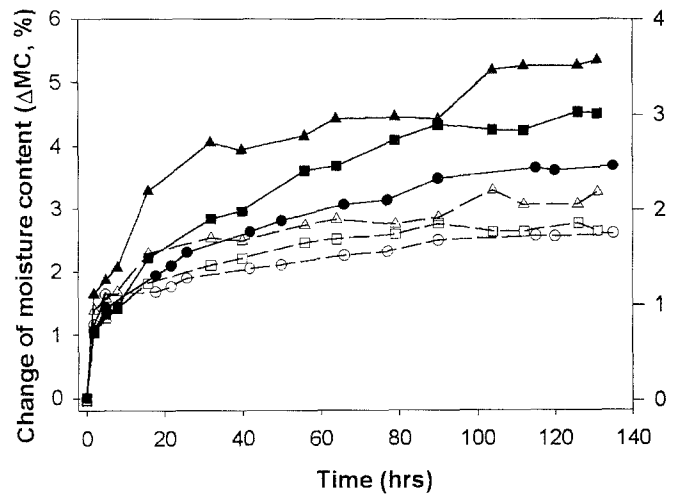


Fig. 2. Change of moisture content (MC) and linear expansion (LE) of hardboard with time at relation humidities (RHs) of 60%–90%. Solid lines,  $\Delta MC$ ; dotted lines, LE; circles,  $a = 200$ mm; squares,  $a = 300$ mm; triangles,  $a = 400$ mm

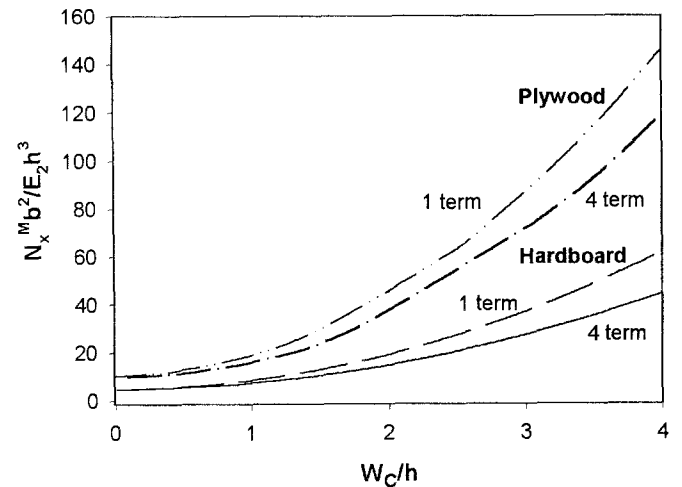


Fig. 3. Nondimensional load-center deflection curves of clamped square panels with immovable edges

### Nondimensional center deflection of square panels with immovable edges

The first four terms in each of the series for  $u$ ,  $v$ , and  $w$  were used for the numerical analysis. Equation (8) gave a set of 12 simultaneous nonlinear equations for  $A_{mn}$ ,  $B_{mn}$ , and  $C_{mn}$ . To solve these equations, Newton's method was adopted because it always converges if the initial approximation is sufficiently close to the solution. It converged within 10 iterations for the present analyses, giving a convergence criterion of  $1 \times 10^{-5}$ . The values for the nondimensional center deflection,  $W_c$ , of square plywood and hardboard were obtained using the first four terms and were compared with those obtained using the first term, as shown in Fig. 3. It was assumed that hardboard was an isotropic, homogeneous panel with a Poisson's ratio of 0.25. For the plywood,

**Table 1.** Physical and mechanical properties of hardboard at 25°C, 60% RH

Mechanical properties	Span 200 mm	Span 300 mm	Span 400 mm
Moisture content (%)	6.79 ± 0.58 (10.68 ± 0.71)	6.73 ± 0.30 (11.25 ± 0.69)	6.46 ± 0.48 (11.81 ± 0.84)
Density (g/cm <sup>3</sup> )	0.97 ± 0.02	0.96 ± 0.02	0.95 ± 0.01
Thickness (mm)	2.94 ± 0.01 (3.05 ± 0.02)	2.91 ± 0.01 (3.02 ± 0.04)	2.92 ± 0.03 (3.08 ± 0.04)
MOE (GPa)	4.57 ± 0.53 (4.02 ± 0.33)	4.22 ± 0.74 (3.72 ± 0.68)	4.38 ± 0.58 (3.86 ± 0.51)
Coefficient of LE (×10 <sup>-3</sup> )	0.461 ± 0.047	0.397 ± 0.096	0.418 ± 0.065

Results are averages of 21 to 28 tests

Numbers in parentheses represent the value at 25°C and 90% RH

RH, relative humidity; MUE, modulus of elasticity; LE, linear expansion

which is one of the typical orthotropic wood-based panels, the assumed  $E_1/E_2$ ,  $G_{12}/E_2$ , and  $\nu_{12}$  values were 5.0, 0.2, and 0.12, respectively.

For the square panel, the coefficient  $C_{11}$  was dominant, and  $A_{21}$  was dominant among  $A_{mn}$ . For hardboard,  $A_{mn}$  was equal to  $B_{mn}$ . Figure 3 showed that the center deflection decreased with increasing MOE. As shown in Fig. 4, maximum tension strain occurred at the midpoint ( $a/2$  and  $b/2$ ) and the compression strain at  $a/2$  and  $b/8$  or  $a/2$  and  $7b/8$ . In addition, the one-term displacement function was chosen to develop the closed-form solution, shown as Eq. (9).

$$u = A \sin \frac{\pi x}{a} \sin \frac{\pi y}{b}, \quad v = B \sin \frac{\pi x}{a} \sin \frac{\pi y}{b}$$

$$w = C \left( \sin \frac{\pi x}{a} \right)^2 \left( \sin \frac{\pi y}{b} \right)^2 \quad (9)$$

Adopting the same procedures, the solution resulted in Eq. (10) and is shown in Fig. 3.

$$C = \frac{8\sqrt{10}}{5\pi} \times \frac{1}{\left( 21b^4A_{11} + 21a^4A_{22} + 10a^2b^2A_{12} + 20a^2b^2A_{66} \right)^{1/2}} \times$$

$$\left[ -\pi^2(12b^4D_{11} + 12a^4D_{22} + 8D_{12}a^2b^2 + 16D_{66}a^2b^2) + 3a^2b^4N_x^M + 3a^4b^2N_y^M \right]^{1/2} \quad (10)$$

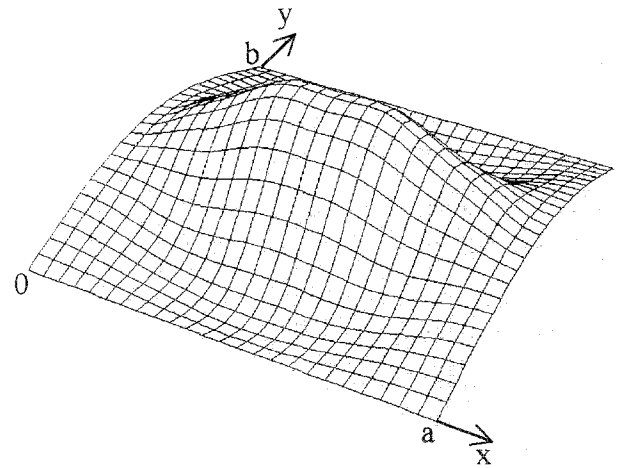
Despite of the differences in the displacement functions, the values of the center deflections obtained using Eq. (10) were almost the same as the one-term solution from Eq. (6). Also, the  $N_{cr}$  values obtained from both Eq. (10) and the four-term Eq. (6) were 4.679 and 4.661 for isotropic square panels, respectively. However, the differences were small.

To determine the influence of using different boundary conditions for the prediction of  $N_{cr}$  and  $W_c$ , the present solutions were compared with Chia's nine-term solutions<sup>3</sup> which were obtained with boundary conditions different from the one used for this work. Chia assumed that the loaded and unloaded edges were uniformly displaced by normal stress. Table 2 shows that the present solutions for

**Table 2.** Comparison of nondimensional center deflection with that of Chia for square plates

$N_u/N_{cr}$	Hardboard		Plywood	
	Present (4.661)	Chia (3.831)	Present (10.024)	Chia (9.407)
1.1	0.438	0.659	0.421	0.789
1.5	0.976	1.546	0.929	2.117
2.0	1.376	2.329	1.293	3.529
2.5	1.681	3.152	1.556	4.879
3.0	1.939	4.161	1.759	6.327

Numbers in parentheses represent the value of the nondimensional critical load,  $N_{cr}$

**Fig. 4.** Typical nonlinear strain,  $\epsilon_x$ , of panels

$N_{cr}$  are slightly larger than Chia's results, but the  $W_c$  values were much less than those of Chia.

#### Postbuckling of the hollow core sandwich panel

Figure 5 shows the experimental and predicted results of the postbuckling of the hollow core type sandwich panel. It was not clear whether test specimens for the sandwich panels were flat during preparation because it was difficult to measure the extent of the initial flatness throughout the

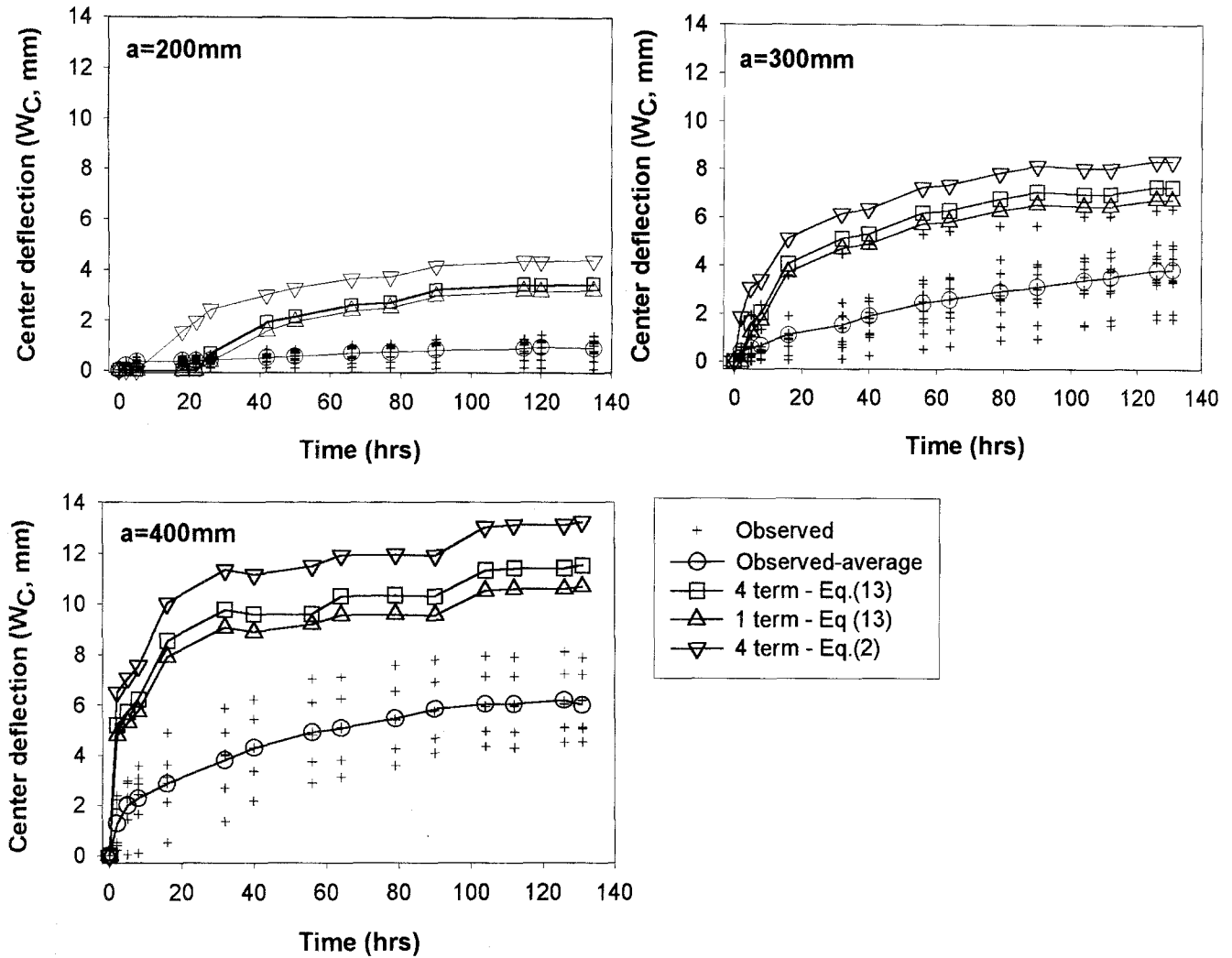


Fig. 5. Comparison of the predicted and observed center deflections of a sandwich panel with movable edges

panel. Therefore, some errors due to the presence of imperfections might have influenced the predicted results. This was evident in the case of the short span ( $a = 200$ ).

The evaluation of  $W_c$  using the nondimensional center deflection for panels with immovable edges is shown in Fig. 3 and was much larger than the observed results. This might be attributed to the in-plane stress whose distribution was uniform in-plane before initial buckling and nonuniform beyond buckling, as shown in Fig. 4. Therefore, its edges might have movements due to hygroexpansion forces on the surface of panel, and the edge movement should be taken into consideration for the prediction to accommodate errors.

The edge movement due to the LE of facing panels can be calculated by modifying the theory of solid laminates.<sup>16</sup> If the LE of the core is ignored and edges are displaced uniformly, it can be represented as Eq. (11).

$$\varepsilon_1 = \frac{2E_1 h \bar{\varepsilon}_x}{2E_1 h + \beta E_c h_c}, \quad \varepsilon_2 = \frac{2E_2 h \bar{\varepsilon}_y}{2E_2 h + \beta E_c h_c} \quad (11)$$

where the average strains in each direction are expressed as

$$\bar{\varepsilon}_x = \frac{1}{ab} \int_0^a \int_0^b \left( \varepsilon_x + \frac{1}{2} \left( \frac{\partial w}{\partial x} \right)^2 - \alpha_x \Delta MC \right) dx dy$$

$$\bar{\varepsilon}_y = \frac{1}{ab} \int_0^a \int_0^b \left( \varepsilon_y + \frac{1}{2} \left( \frac{\partial w}{\partial y} \right)^2 - \alpha_y \Delta MC \right) dx dy \quad (12)$$

Therefore, the effective hygroexpansion forces are given as

$$N_x^M = (\alpha_x \Delta MC - \varepsilon_1) A_{11} + (\alpha_y \Delta MC - \varepsilon_2) A_{12}$$

$$N_y^M = (\alpha_x \Delta MC - \varepsilon_1) A_{21} + (\alpha_y \Delta MC - \varepsilon_2) A_{22} \quad (13)$$

The average strain that contributed to the edge movement was represented as a function of LE in Fig. 6 in which the MOEs parallel to the grain and perpendicular to the grain of the LVL core were assumed to be 10.0 and 0.5 Gpa, respectively. As expected, the average strain was inversely

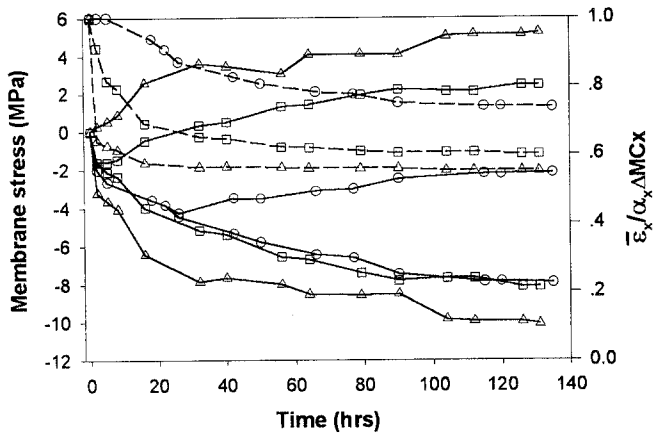


**Fig. 6.** Predicted maximum and minimum membrane stress ( $\sigma_x$ ), and ratio of average strain to LE of sandwich panels with movable edges. *Solid lines*, membrane stress; *dotted lines*, ratio of average strain to LE; *circles*,  $a = 200$  mm; *squares*,  $a = 300$  mm; *triangles*,  $a = 400$  mm

proportional to the span and decreased as deflections increased. The center deflections obtained by considering the edge movement by Eq. (13) were closer to the average observed than those by Eq. (1), but all the predicted results overestimated them. The reason might be the plastic deformation at high MC and high stress level,<sup>18</sup> as shown in Fig. 6. It was clear from the results that the errors increased as the span increased because membrane stress was inversely proportional to the edge movement. In the cases of  $a = 300$  and  $400$  mm, it was estimated that tensile stress occurred at both points  $a/2$  and  $b/2$ .

**Postbuckling of a strip with immovable edges**

The first five terms in each of the series of Eq. (7) were used to predict the center deflection and membrane stress. Similarly, Newton's method was used to solve a set of 10 simultaneous nonlinear equations for the panels. The analysis showed that the coefficient  $C_1$  was most dominant, and  $A_2$  was dominant among  $A_m$ . The rest of the coefficients, except  $C_1$  and  $A_2$ , were close to zero.

Buckling stresses for span lengths of 200, 300, and 380 mm were 3.5, 1.4, and 0.91 MPa, respectively. The stress increased as the hygroexpansion increased in the panel, but there was little change beyond the buckling of the strips.

The center deflections predicted by Eqs. (7) and (8) were independent of the MOE, which was different from that of sandwich panels. It was almost the same as those of the measured deflection, as shown in Fig. 6, particularly for span lengths 300 and 400 mm. However, with a span length of 200 mm the predicted deflection was larger than the measured result, which could be attributed to the plastic deformation of a large buckling stress and the center deflection beyond buckling.

The center deflection due to hygroexpansion can be also calculated.<sup>4,17</sup> To understand the postbuckling behavior, another equation can be derived using the relation between  $R$  and  $\epsilon$ , as shown in Eq. (14):

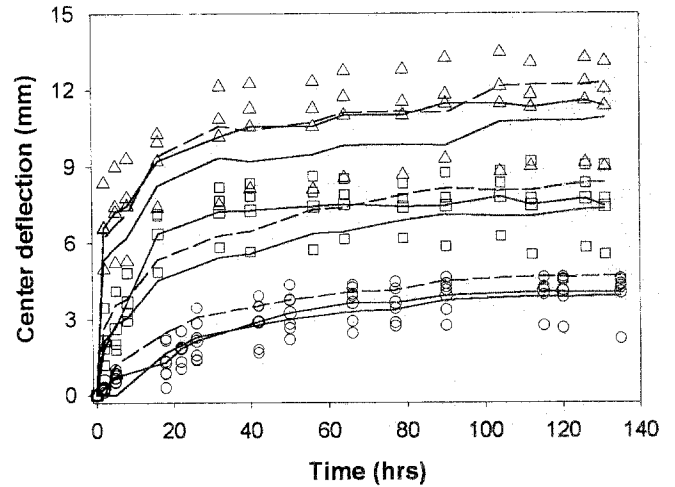


**Fig. 7.** Comparison of the predicted and observed center deflections of a strip. *Solid lines*, Eq. (16); *dotted lines*, Eqs. (7) and (8); *solid lines and symbols* are averages; *circles*,  $a = 200$  mm; *squares*,  $a = 300$  mm; *triangles*,  $a = 400$  mm

$$s = a + \Delta a = 2R\theta$$

$$\theta = \sin^{-1} \frac{a}{2R}$$

$$s = 2R \sin^{-1} \frac{a}{2R}$$

$$\therefore 1 + \epsilon = \frac{2R}{a} \sin^{-1} \frac{a}{2R} \tag{14}$$

Assuming that once a critical load is reached and the strip is incapable of supporting any further hrs load, the strain is given as:

$$\epsilon = \alpha_x \Delta MC - \frac{\pi^2 h^2}{3a^2} \tag{15}$$

Therefore, the center deflection can be calculated by replacing the  $R$  value given by Eqs. (14) and (15) with Eq. (16). The calculated value is about 4% smaller than Spalt's result.<sup>17</sup>

$$w_{x=a/2} = \frac{1}{8} \frac{a^2}{R} \tag{16}$$

The center deflections obtained by the above equations are represented in Fig. 7. The results show the same trend as those obtained by the Rayleigh-Riz method, but the former were somewhat smaller than the latter, which might be due to the effects of Poisson's ratio. Therefore, this result suggests that all hygroexpansion forces are not stored in the strips but contribute to the deflection after buckling begins. In addition, this result indicates that the postbuckling behavior of the strips differs greatly from that in the panel.

**Conclusions**

This study was carried out to investigate postbuckling behavior of wood-based sandwich panels under various envi-

ronmental conditions. For the model development of postbuckling behavior, a few assumptions were made, including the free hygroexpansion that could be converted into elastic strain, the ignoring of imperfections, the time-dependent creep, and relaxation phenomena. Taking the edge movement of hardboard fixed on the core into consideration resulted in some discrepancy between theoretical and experimental results of the center deflection, and the theoretical value showed a slight overestimate because of neglecting the plastic deformation. This study showed that there was a large difference in the postbuckling behavior between panels and strips. The postbuckling behavior of panels depended on the MOE, while the behavior of strips was independent of MOE. Furthermore, the in-plane load of the panel increased beyond buckling, but the load for strips was constant with the initial buckling load. Further studies are necessary to improve the accuracy of the developed model on buckling and postbuckling, including the viscoelasticity dealing with stress changes with time and the development of a more sophisticated model that accommodates the plastic deformation of panels and the nonuniform edge movements.

### Appendix: abbreviations and symbols

$\Pi$	total potential energy of panel
$A_{ij}, D_{ij}$	extensional and bending stiffness, respectively
$\varepsilon_x, \varepsilon_y$	midplane strains in $x$ and $y$ directions, respectively
$\gamma_{xy}$	midplane shear strain in $xy$ plane
$N_x^M, N_y^M$	hygroscopic forces in $x$ and $y$ directions, respectively
$h$	panel thickness
$a, b$	panel length in $x$ and $y$ directions, respectively
$x, y, z$	coordinate system
$u, v, w$	displacement in $x, y,$ and $z$ directions, respectively
$\Delta MC$	moisture content change
$\alpha_x, \alpha_y$	coefficient of linear expansion in $x$ and $y$ directions, respectively
$LE$	linear expansion ( $\alpha \Delta MC$ )
$s$	arc length
$R$	radius of curvature
$N_x, N_y$	resultant in-plane forces per unit length in $x$ and $y$ directions, respectively

$N_n$	nondimensional load, $N_x^M b^2/E_2 h^3$
$N_{cr}$	nondimensional critical load, $N_{x,cr}^M b^2/E_2 h^3$
$\beta$	ratio of the core to the total width, $a_c/a + a_c$
$E_c$	effective core MOE, $E_{  } + E_{\perp}$ (i.e., the summation of MOE parallel to the grain and perpendicular to the grain)
$h_c$	core thickness

### References

1. Yamazoe M, Sadoh T (1993) Predicting moisture content fluctuations of wood accompanying the weather and seasonal changes of atmosphere. *Mokuzai Gakkaishi* 39:788–794
2. Leissa AW (1987) A review of laminated composite plate buckling. *Appl Mech Rev ASME* 40:575–591
3. Chia CY, Prabhakara MK (1974) Postbuckling behavior of unsymmetrically layered anisotropic rectangular plates. *J Appl Mechanics March*:155–162
4. Rao GV, Raju KK (1984) Thermal postbuckling of columns. *AIAA J* 22:850–851
5. Tauchert TR (1991) Thermally induced flexure, buckling, and vibration of plates. *Appl Mech Rev ASME* 44:347–360
6. Noor AK, Burton WS (1992) Computational models for high-temperature multilayered composite plates and shells. *Appl Mech Rev ASME* 45:419–445
7. Raju KK, Rao GV (1989) Thermal post-buckling of thin simply supported orthotropic square plates. *Composite Struct* 12:149–154
8. Myers CA, Hyer MW (1991) Thermal buckling and postbuckling of symmetrically laminated composite panels. *J Thermal Stress* 14:519–540
9. Feldman E, Aboudi J (1995) Thermal postbuckling of metal matrix laminated plates. *J Thermal Stress* 18:197–218
10. Librescu L, Lin W, Nemeth MP, Starnes JH (1995) Thermomechanical postbuckling of geometrically imperfect flat and curved panels taking into account tangential edge constraints. *J Thermal Stress* 18:465–482
11. Shen HS, Lin ZQ (1995) Thermal post-buckling analysis of imperfect laminated plates. *Comput Struct* 57:533–540
12. Shen HS (1998) Thermomechanical post-buckling analysis of imperfect laminated plates using higher-order shear-deformation theory. *Comput Struct* 66:395–409
13. Tauchert TR (1986) Thermal stresses in plates – statistical problems. In: Hetnarski RB (ed) *Thermal stresses I*. Elsevier Science, Amsterdam, p 123
14. Jones RM (1975) *Mechanics of composite materials*. Scripta Book Company, pp 239–259
15. Chia CY (1980) *Nonlinear analysis of plates*. McGraw-Hill, New York, pp 158–166
16. Suchsland O (1990) Estimating the warping of veneered furniture panels. *For Prod J* 40(9):39–43
17. Spalt HA, Sutton RF (1968) Buckling of thin surfacing materials due to restrained hygroexpansion. *For Prod J* 18(4):53–56
18. Suchsland O, Xu D (1992) Determination of swelling stresses in wood-based materials. *For Prod J* 42(5):25–27